Int J Adv Manuf Technol (2013) 69:2471–2480
DOI 10.1007/s00170-013-5190-8

ORIGINAL ARTICLE

Experimental modeling and optimization of electric discharge diamond face grinding of metal matrix composite

Pankaj Kumar Shrivastava · Avanish Kumar Dubey

Received: 16 February 2012 / Accepted: 8 July 2013 / Published online: 7 August 2013

Abstract Machining of metal matrix composites (MMCs) has been a big challenge for manufacturing industries due to its superior mechanical properties. Unconventional machining methods have become an alternative to give desired shapes with intricate profiles and stringent design requirements. The present research investigates the grinding performance of copper–iron–graphite MMC using electric discharge diamond face grinding (EDDFG), which is electric discharge machining-based hybrid machining process. Experiments have been performed on a self-developed experimental setup of EDDFG with scientifically designed experiments. Effects of process input parameters on two important performances, material removal rate (MRR) and surface roughness (SR), have been analyzed. Genetic algorithm-based optimization of MRR and SR models show considerable improvements in both characteristics, as confirmed by verification experiments. Results reveal that peak current is a common significant factor for both MRR and SR.

Keywords Metal matrix composite · Electric discharge diamond face grinding · Material removal rate · Surface roughness · Genetic algorithm · Optimization

1 Introduction

Metal matrix composites (MMCs) are in great demand in the modern manufacturing industries due to its improved technological characteristics such as high strength/weight ratio, hot hardness, and corrosion and wear resistance [1, 2]. Due to enhanced mechanical properties, conventional machining methods experience difficulties in machining these materials. The unconventional machining processes are suitable for shaping advanced difficult-to-cut materials with certain limitations. The electric discharge machining (EDM) is such an unconventional machining process used in modern manufacturing industries for machining electrically conductive difficult-to-cut materials [3, 4].

A lot of research work has been done and is still going on to explore the potential of EDM during machining of conventional as well as difficult-to-cut materials. Ozgedik and Can [5] performed an experimental study on steel workpiece under varying current and flushing conditions to examine the variations of material removal rate (MRR), tool wear rate (TWR), and surface roughness (SR). They found increasing trends in the MRR, TWR, and SR with the increase in discharge current. They also reported that injection flushing produces better surface quality but higher TWR, while suction flushing gives maximum MRR. Kansal et al. [6] optimized the process parameters of powder-mixed EDM using response surface methodology. They found positive effects on MRR and SR by adding the silicon powder. They also identified peak current and silicon powder concentration as the most significant control factors.

Lauwers et al. [7] investigated the material removal mechanism of electrically conductive ceramic materials by analysis of the debris and surface/sub-surface quality. They concluded that beside melting and vaporization, the material removal also occurs due to oxidation and dissolution of the base material. Ramulu et al. [8] investigated the EDM effect on the mechanical properties of whisker-SiC_p aluminum MMC and SiC_p/A356 aluminum MMC. They observed that EDM sparking reduces fatigue and ultimate strength by 15–25 %. Mohan et al. [9] investigated EDM performance of SiC/Al composite using rotary tube electrode and found that peak current, polarity, pulse duration, hole diameter, speed of rotation of electrode, and volume fraction of SiC-reinforced particles have significant effects on MRR, TWR, and SR.

P. K. Shrivastava · A. K. Dubey (✉)
Mechanical Engineering Department, Motilal Nehru National Institute of Technology, Allahabad 211004, Uttar Pradesh, India
e-mail: avanishdubey@yahoo.com

Poor machining efficiency in terms of low MRR, tool wear, and high-specific energy of EDM restricts its further applications. To address these problems, hybrid machining processes are now gaining importance. The advantages of both conventional and unconventional machining processes can be utilized together by using hybrid machining processes. Ji et al. [10] proposed such an innovative hybrid machining process that combines end electrical discharge milling (EDML) and grinding for machining silicon carbide ceramics. They claimed that combined process is highly efficient and cost effective in machining large surface area. They also claimed that there is considerable improvement in the process performances such as MRR, TWR, and surface integrity as compared to pure electrical discharge milling. Ji et al. [11, 12] elucidated the effects of input control factors such as tool polarity, peak current, peak voltage, pulse-on time and pulse-off time on the MRR, TWR, and SR during combined EDML and grinding of silicon carbide ceramics. They also found significant control factors and developed mathematical models for the above mentioned quality characteristics. Furthermore, they found optimum values of the input control factors to improve the quality characteristics. In another work, Ji et al. [13] observed the surface microstructure of silicon carbide ceramics machined by combined EDML and grinding. The analysis by scanning electron microscope, x-ray diffraction, and energy dispersive spectrometer revealed that finish machining mode results in better surface integrity than that in rough machining mode.

Electric discharge abrasive grinding (EDAG) is another EDM-based hybrid machining process which utilizes synergistic interactive effect of EDM and conventional grinding. In EDAG, metal-bonded abrasive wheel is used as tool electrode. The whole workpiece and part of the wheel is submerged in the dielectric and the spark is generated between the metal bond and the workpiece [3]. The spark in EDAG (Fig. 1a) plays three roles: firstly, it does continuous dressing of the wheel so that active grains are continuously exposed and the wheel doesn't clog; secondly, it softens the workpiece so the grain easily removes the material; and thirdly, it may actually remove substantial amount of material through melting and vaporization. The EDAG can be operated in three different configurations i.e., electric discharge abrasive surface grinding, electric discharge abrasive cut-off grinding, and electric discharge abrasive face grinding. If diamond is used as abrasive, then EDAG is known as electric discharge diamond grinding (EDDG). In EDAG, the grain protrusion height P_h and inter-electrode gap g_w (Fig. 1b) are very important parameters which significantly affect the performance parameters, as these directly control the depth of penetration (P_h–g_w) of abrasive grain [14].

The performance of EDAG depends on many electrical and non electrical input parameters. The proper control of these parameters gives better performance such as high surface quality, high MRR and low wheel wear rate (WWR). Jain et al. [14] carried out experimental study on electric discharge diamond cut-off grinding (EDDCG) of high-speed steel with varying current, voltage, pulse-on time, and duty factor (DF). They found that MRR increases with the increase in the current or pulse-on time, and decreases with increase in the voltage or DF. Similarly, the normal force decreases with increase in current, voltage or DF. Koshy et al. [15] presented the mechanism of material removal in EDDCG using high-speed steel workpiece. They elucidated the role of current and wheel speed on MRR, grinding forces, and power. They reported considerable improvement in the process performance as compared to EDM due to thermal softening and continuous in-process dressing and declogging of the wheel surface. Kumar and Choudhury [16] performed EDDCG experiments on the high-speed steel using central rotatable composite design of experiments and developed response models for WWR and SR. Using these models, they generated training data for the artificial neural network (ANN) and found that ANN model suitably predict the EDDCG process behavior. Chandrasekhar et al. [17] elucidated the effect of input parameters such as discharge current, pulse-on time, pulse-off time, and wheel speed on the MRR and SR during electric discharge face grinding of high-carbon steel and HSS workpiece. They found that both MRR and surface finish improved by use of rotating wheel as compared to the stationary wheel or electrode. Koshy et al. [18] carried out EDDCG of cemented carbide with varying current and pulse-on time. It was found that discharge

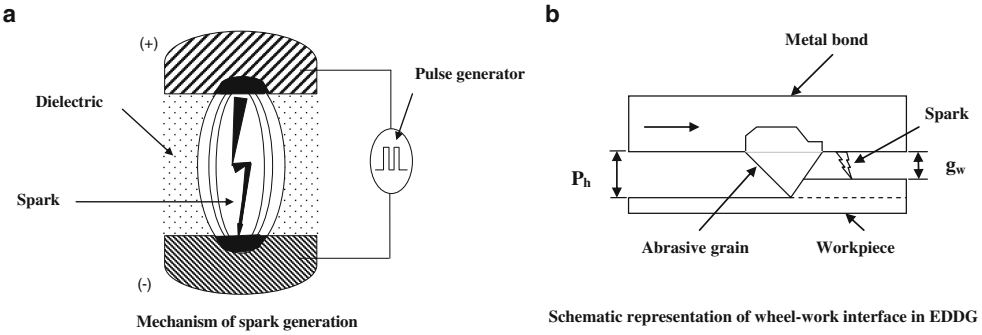

Fig. 1 Schematic diagram of EDDG. **a** Mechanism of spark generation. **b** Schematic representation of wheel-work interface in EDDG

enhances the grinding performance by increasing the MRR and decreasing the grinding forces. Singh et al. [19] performed electric discharge diamond face grinding (EDDFG) experiments on tungsten carbide–cobalt composite by considering wheel speed, peak current, pulse-on time, and DF as process input parameters. The quality characteristics considered were MRR, WWR, and SR. They found that wheel speed is the most significant factor which affects the process performance during EDDFG of tungsten carbide–cobalt composite. They also suggested optimum process parameters using gray relational analysis. Shrivastava et al. [20] developed the computer-aided-hybrid-neural-GA software for ANN modeling and genetic algorithm (GA) optimization of EDDG process. They applied this software for modeling and optimization of MRR and average temperature during EDDG of high-speed steel. They claimed considerable improvement in both quality characteristics.

It is evident from the review of literature presented that most of the research works in the area of EDM and EDAG were focused on machining of metals and alloys. Few works reported on MMCs were mainly concentrated on aluminum-based MMCs. Authors could not find any work on EDM or EDAG of copper–iron–graphite composite. In the present research, an attempt has been made to develop the EDDG setup with rotating wheel and study the process performance of copper–iron–graphite MMC by analyzing MRR and SR. The effects of input parameters such as peak current, pulse-on time, pulse-off time, and grit size on output characteristics MRR and SR have been analyzed by developing response models. The MRR and SR models have been optimized using GA-based artificial intelligence tool. The predicted optimum results have been verified by confirmation experiments.

2 Methodology

2.1 Taguchi methodology

Taguchi methodology (TM) is a widely acknowledged and accepted method of robust parameter design. In this method, main process parameters or control factors which influence process results are taken as input parameters and the experiment is performed as per specially designed orthogonal arrays. Orthogonal arrays are two-dimensional arrays of numbers which have the interesting quality that by choosing any two columns in the array, one can receive an even distribution of all the pair-wise combinations of values in the array. Orthogonal array offers many benefits. Compared to conventional experimental design, the TM-based orthogonal array examined the quality characteristics through a minimum number of experiments so there is a large saving in experimental efforts and data analysis is also easier. The selection of appropriate orthogonal array is based on the total degree of freedom which is computed as [21] follows:

$$\begin{aligned}\text{Degree of freedom} = {} & (\text{number of levels}-1)\,\text{for each factor} \\ & + (\text{number of levels}-1) \\ & \times (\text{number of levels}-1) \\ & \quad \text{for each interaction} + 1.\end{aligned}$$

2.2 Response surface methodology

Response surface methodology (RSM) is a collection of mathematical and statistical techniques that are useful for the modeling and analysis of problems in which a response of interest is influenced by several variables. RSM quantifies the relationship between the controllable input parameters and the obtained responses [22]. In modeling and optimization of manufacturing processes using RSM, the sufficient data is collected through scientifically designed experiments.

In RSM, the relation between the process performance and process input parameters is expressed as

$$y = f\left(x_1, x_2, x_3, \ldots\ldots\ldots\ldots x_p\right), \tag{1}$$

Where, x_1, x_2, x_3,……., x_p are input process parameters and y is the process performance or desired quality characteristic. By plotting the expected response of y, a surface, known as the response surface, is obtained. The form of f is unknown and may be very complicated. Thus RSM aims at approximating f by a suitable lower-order polynomial in some region of the input process parameters. Usually, a second order regression model, which includes curvature effect, is utilized in RSM

$$y = b_o + \sum_{i=1}^{p} b_i x_i + \sum_{i=1}^{p} b_{ii} x_i^2 + \sum_i \sum_j b_{ij} x_i x_j \tag{2}$$

Where, $b_o$is constant and all b's are regression coefficients determined by the least square method using the following equation:

$$b = \begin{bmatrix} b_0 \\ b_1 \\ \ldots \\ \ldots \\ b_n \end{bmatrix} = \left(x^T x\right)^{-1} x^T y \tag{3}$$

Where x^T is the transpose of matrix x and $(x^T x)^{-1}$ is the inverse of matrix $x^T x$.

2.3 Genetic algorithm

GA is quite suitable to solve the optimization models that are nonlinear and complex. It is based on Darwin's principle of natural selection and the concepts of natural genetics, especially "survival of the fittest." GA is able to search very large solution spaces

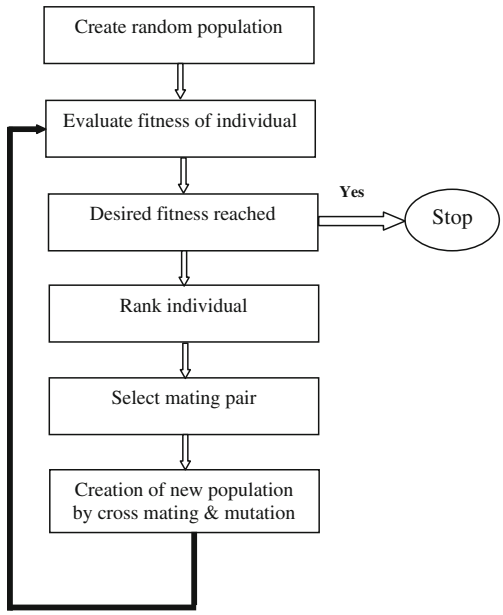

Fig. 2 Flowchart for genetic algorithm

efficiently by providing a lower computational cost, since they are a probabilistic transition rules instead of deterministic ones and most effectively applied to problems in which small changes result in very non-linear behavior in the solution space [23].

The mechanism of GA is simple, involving copying of binary strings. The computations are carried out in three stages to get a result in one generation or iteration. The working of GA has been shown with the help of block diagram in Fig. 2 [24]. The searching process mimics the natural evolution of biological creatures and turns out to be an intelligent exploitation of a random search. In GA, the control factors are typically encoded into a string (binary coding) or chromosome structure. GA begin with a population of strings (individuals) created at random. The fitness of each individual string is evaluated with respect to the given objective function. Then, this initial population is operated by three main operators: reproduction, crossover, and mutation to create a better population. Highly fit individuals or solution are given opportunities to reproduce by exchanging pieces of their genetic information in the crossover procedure with other highly fit individuals. This produces new "offspring" solutions, which shares some characteristics taken from both the parents. Mutation is often applied after crossover by altering some genes in the offspring. This new population is further evaluated and tested for some termination criteria. The reproduction–crossover–mutation–evaluation cycle is repeated until the termination criteria are met.

3 Experimental details

3.1 Development of experimental setup

The EDDFG setup (Fig. 3) has been developed and attached to the ELEKTRA PULS die sinking spark erosion machine. The setup consists of a shaft which holds the metal-bonded diamond grinding wheel. The shaft was rotated by a D.C. motor, through a belt and pulley arrangement. The designing of shaft and fixture and selection of motor, bearing, pulley and belt were done by considering all the design principles. Whilst machining, the rotating wheel is fed downwards, towards the work, under the servo control of the EDM machine. The down-feed of the wheel is regulated automatically by the servo control such that

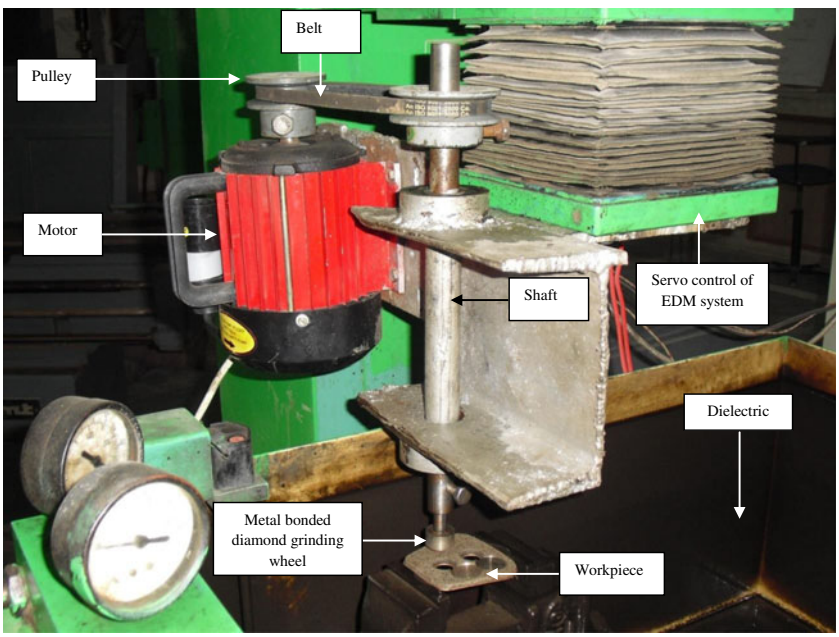

Fig. 3 Experimental setup for electric discharge diamond face grinding

Table 1 Chemical composition of workpiece (%volume)

Copper	Iron	Graphite
60	30	10

the metallic bond and the work are physically separated by a gap, the magnitude of which depends on the local breakdown setting of the dielectric for a particular voltage setting.

The straight polarity has been used throughout the experiments. The workpiece selected is copper–iron–graphite MMC. The composition of the workpiece is shown in Table 1. Three different metal-bonded diamond grinding wheels have been selected to perform the experiments. The specifications of wheels are shown in Table 2.

3.2 Orthogonal array experiments

This study considered four potential factors: peak current, pulse-on time, pulse-off time, and grit number as input parameters, each at level three (Table 3). The wheel speed was kept constant at 900 rpm. The range of the process parameters were decided by extensive pilot experiments. The total degree of freedom, without considering interaction is (3–1)×4+1=9 so a minimum of nine experiments are required as per orthogonal array; however, to get higher resolution, L_{27} orthogonal array was selected. Degree of freedom for experiments is 26. Each experiment was performed for 30 min and amount of material removed was obtained by finding mass difference before and after machining using precision electronic digital weight balance with 0.1-mg resolution. The MRR (in grams per minute) was calculated by the following formula:

$$MRR = \frac{m_f - m_i}{t_p} \tag{4}$$

Where m_i is the initial mass of workpiece (before machining), and m_f is the final mass of workpiece in gram (after machining); t_p is machining time in minutes. The SR was measured using Talysurf Surtronic 25 using a cut-off value of 0.8 mm for each machined specimen. The observed qualities values that are MRR and SR have been tabulated in Table 4.

Table 2 Specification of grinding wheel

Abrasive	Grit No	Concentration (%)	Bond material	Wheel diameter (mm)
Wheel 1 Diamond	80/100	75	Bronze	22
Wheel 2 Diamond	120/140	75	Bronze	22
Wheel 3 Diamond	240/270	75	Bronze	22

Table 3 Control factors and their levels

Factors	Peak current (A)	Pulse-on time (μs)	Pulse-off time (μs)	Grit No.
Symbol	x_1	x_2	x_3	x_4
Level 1	2	10	15	80
Level 2	4	20	20	120
Level 3	6	30	25	240

4 Analysis of material removal rate

4.1 Modeling

Equation 5 shows the second order response model for MRR. It has been developed by using the data of all 27 runs as given in Table 4. The results of analysis of variance (ANOVA) for model MRR is shown in Table 5. The model F value 29.02 implies that the quadratic model is statically

Table 4 Experimental observation for MRR and SR using L_{27} OA

Experiment No.	Control factors				MRR (g/min)	SR (μm)
	x_1	x_2	x_3	x_4		
1	1	1	1	1	0.0604	1.1
2	1	1	2	2	0.0541	0.9
3	1	1	3	3	0.0463	0.87
4	1	2	1	2	0.0629	0.94
5	1	2	2	3	0.0663	0.92
6	1	2	3	1	0.0671	1.30
7	1	3	1	3	0.0622	1.35
8	1	3	2	1	0.0814	1.42
9	1	3	3	2	0.0574	1.33
10	2	1	1	2	0.0984	1.42
11	2	1	2	3	0.0830	1.38
12	2	1	3	1	0.0863	0.89
13	2	2	1	3	0.0904	0.84
14	2	2	2	1	0.0971	1.39
15	2	2	3	2	0.0812	0.94
16	2	3	1	1	0.1081	1.35
17	2	3	2	2	0.0937	1.27
18	2	3	3	3	0.0837	1.46
19	3	1	1	3	0.1030	1.42
20	3	1	2	1	0.1077	1.53
21	3	1	3	2	0.0942	1.46
22	3	2	1	1	0.1157	1.68
23	3	2	2	2	0.1080	1.56
24	3	2	3	3	0.1037	1.40
25	3	3	1	2	0.1033	1.77
26	3	3	2	3	0.1041	1.62
27	3	3	3	1	0.1147	1.93

Table 5 Analysis of variance for MRR model

Source	Degree of freedom	Seq SS	Adj SS	Adj MS	*F* value	*p* Value
Regression	14	0.010448	0.010448	0.000746	29.02	0.000
Linear	4	0.009659	0.000757	0.000189	7.36	0.003
Square	4	0.000657	0.000657	0.000164	6.39	0.005
Interaction	6	0.000132	0.000132	0.000022	0.86	0.552#
Residual error	12	0.000309	0.000309	0.000026		
Total	26	0.010757				
S=0.005071	R-Sq=97.1	R-Sq (adj)=93.88				

#Not significant

significant. There is negligible chances that a model *F* value of this much magnitude could occur due to noise. The value of coefficient of determination R^2 and adjusted R^2 are 97.1 and 93.88, respectively, which means a very high percent of the variation in the response variable can be explained by the explanatory variable. The negligible variation can be explained by unknown or inherent variability. The *S* value of the regression analysis is 0.005071, which is smaller. The associated *p* value for the model, as well as linear and square term, is lower than 0.05 (i.e. α=0.05, or 95 % confidence) indicates that the model is considered to be statistically significant. Further ANOVA of MRR (Table 6) identifies peak current as most significant factor affecting MRR followed by grit size, pulse-on time, and pulse -off time.

The final response surface equation for MRR (in grams per minute), after removing the non-significant terms is given as follows:

$$\begin{aligned} MRR = {} & 0.01257 + 0.02556x_1 + 0.001368x_2 - 0.003825x_3 \\ & - 0.0005197x_4 - 0.001820x_1^2 - 0.00002362x_2^2 \\ & - 0.0001152x_3^2 + 0.000001121x_4^2 \end{aligned} \quad (5)$$

Experimental results show that composite can be effectively machined by EDDFG. High-electrical conductivity and low-thermal resistance of all the constituents of composite promotes good MRR. Figure 4 shows the estimated response surface for MRR in relation to the design parameters of peak current and grit size since these parameters have the most significant influence on MRR. It can be seen that for the given range of peak current, the MRR tends to increase considerably with increase in peak current. It may be due to different reasons. The increase in the peak current increases input energy, since more numbers of electrons per unit time collides with the workpiece so there is more conversion of kinetic energy of electrons into heat energy. If EDDFG is grinding dominated, then there will be more softening of the workpiece surface which will result to more removal of material by abrasive grains. Even if it is EDM dominated, there will be more MRR due to melting and vaporization. Also, as the current increases, the wheel wear increases; so more numbers of active grains are exposed and also the depth of penetration of active grain (P_h–g_w) increases, so MRR increases. As the grit number increases, the MRR decreases since, with the increase in the grit number, the grain size decreases which results in smaller depth of cut [25] and hence MRR decreases.

Table 6 Analysis of variance for material removal rate

Source	Degree of freedom	Sum of square	Mean square	*F* value	Contribution (%)
Peak current	2	0.00904	0.00452	184.49	87.6
Pulse-on time	2	0.00035	0.00017	7.08	3.4
Pulse-off time	2	0.00032	0.00016	6.52	3.1
Grit No	2	0.00061	0.00031	12.45	5.9
Error	18	0.00044	0.00002		
Total	26	0.01076			

4.2 Optimization

The standard optimization problem definition requires an objective function to be minimized or maximized and may require the constraint functions to be satisfied in term of optimization parameters. In the present case, the objective function of optimization problem can be stated as below:

Find: x_1,x_2,x_3 and x_4

Maximize:

$$\begin{aligned} MRR = {} & 0.01257 + 0.02556x_1 + 0.001368x_2 - 0.003825x_3 \\ & - 0.0005197x_4 - 0.001820x_1^2 - 0.00002362x_2^2 \\ & - 0.0001152x_3^2 + 0.000001121x_4^2 \end{aligned} \quad (6)$$

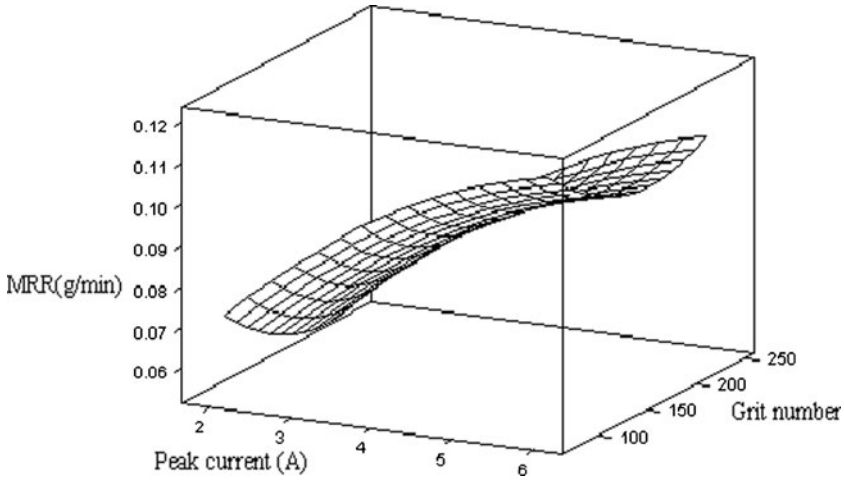

Fig. 4 Effect of peak current and grit number on MRR (hold values: pulse-on time=20 μs and pulse-off time=20 μs)

With range of process input parameters:

$$2 \le x_1 \le 6$$
$$10 \le x_2 \le 30$$
$$15 \le x_3 \le 25$$
$$80 \le x_4 \le 240$$

The critical parameters of GA are the size of the population, mutation rate, cross-over rate, and number of generations. After trying different combinations of GA parameters, the population size 40, cross-over rate 1.0, mutation rate 0.01, and number of generation 50, have been taken for MRR. The objective function in Eq. (6) has been solved without any constraint. In Fig. 5, the best and mean fitness curves are illustrated in the search space. The fitness function is optimized when the mean curve converges to the best curve after 15 generations. The corresponding values of control factors peak current, pulse-on time, pulse-off time, and grit number have been found as 5.99 A, 29.81 μs, 15.05 μs, and 80, respectively. Hence these are the optimum values of control factors. Using these values, the value of MRR has been obtained as 0.1183 g/min.

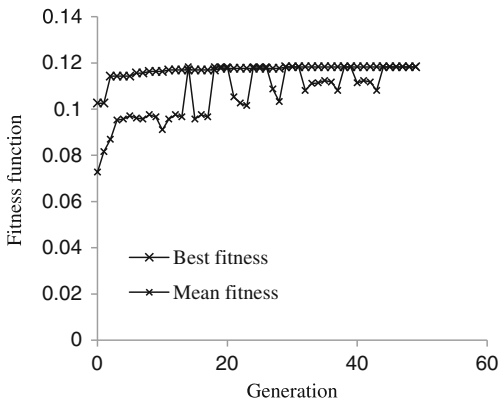

Fig. 5 Generation-fitness function graphics for MRR

5 Analysis of surface roughness

5.1 Modeling

Equation (7) shows the second order response model for SR. It has been developed by using data of all 27 runs as given in Table 4. The results of ANOVA for model SR is shown in Table 7. The model F value 24.37 implies that the quadratic model is statically significant. There is negligible chances that a model F value of this much magnitude could occur due to noise. The value of coefficient of determination R^2 and adjusted R^2 are 96.6 and 92.6, respectively, which means a very high percent of the variation in the response variable can be explained by the explanatory variable. The negligible variation can be explained by unknown or inherent variability. The S value of the regression analysis is 0.08025, which is smaller. The associated p value for the model and square term is lower than 0.05 (i.e., α=0.05, or 95 % confidence) which indicates that the model is considered to be statistically significant. ANOVA of SR (Table 8) identifies peak current as most significant factor affecting SR followed by pulse-on time, grit size, and pulse-off time.

The final response surface equation for SR (in micrometer), after removing the non-significant terms is given as follows:

$$\begin{aligned} SR = {} & 2.3961 - 0.2013x_1 - 0.0103x_2 - 0.0552x_3 - 0.008697x_4 \\ & + 0.03986x_1^2 + 0.0007111x_2^2 + 0.001578x_3^2 \\ & + 0.00002182x_4^2 \end{aligned} \quad (7)$$

Although the linear terms are non-significant, they have been included in the response surface equation following the hierarchy principle. The hierarchy principle indicates that if a model contains a higher-order term, it should also contain all the lower-order terms that compose it [22]. The variation in the SR with the peak current and pulse-on time is shown in the response surface plot (Fig. 6). It is evident that as current

Table 7 Analysis of variance for SR model

Source	Degree of freedom	Seq SS	Adj SS	Adj MS	*F* value	*p* Value
Regression	14	2.197	2.197	0.1569	24.37	0.000
Linear	4	1.8985	0.0625	0.01562	2.42	0.105#
Square	4	0.25295	0.25295	0.06324	9.82	0.001
Interaction	6	0.04636	0.04636	0.007726	1.2	0.370#
Residual error	12	0.07731	0.07731	0.0064		
Total	26	2.27512				
S=0.08025	R-Sq=96.6	R-Sq (adj)=92.6				

#Not significant

Table 8 Analysis of variance for surface roughness

Source	Degree of freedom	Sum of square	Mean square	*F* value	Contribution (%)
Peak current	2	1.14659	0.57329	83.44	53.3
Pulse-on time	2	0.62076	0.31038	45.18	28.85
Pulse-off time	2	0.03734	0.01867	2.72	1.73
Grit No	2	0.34676	0.17338	25.24	16.12
Error	18	0.12367	0.00687		
Total	26	2.27512			

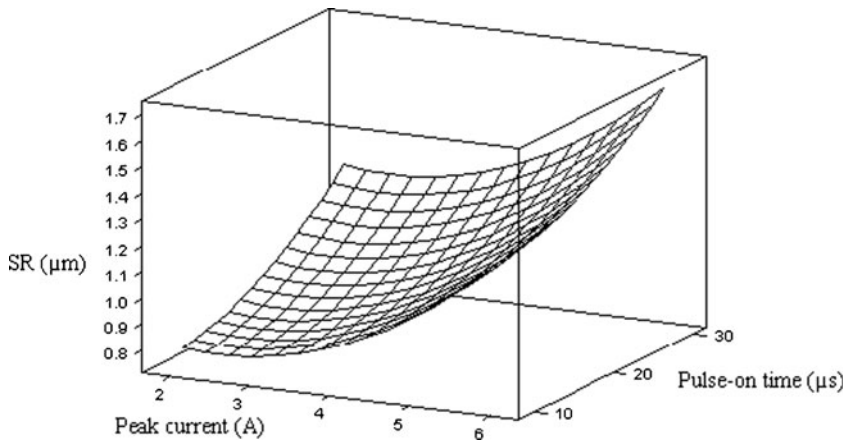

Fig. 6 Effect of peak current and pulse-on time on SR (hold values: pulse-off time=20 µs and grit number=120)

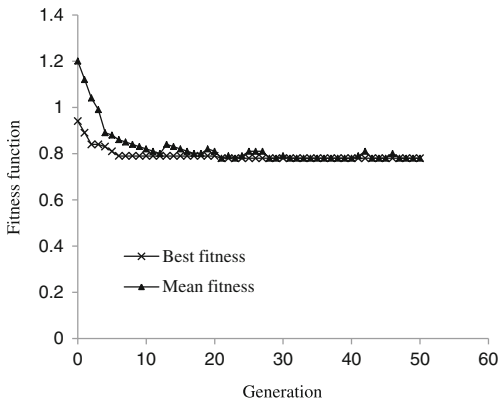

Fig. 7 Generation-fitness function graphics for SR

increases, the SR increases. The increase in current increases the input energy, which in turn, leads to formation of bigger craters in the workpiece, so SR increases. Also, with the increase in peak current, the depth of penetration of active grain increases which generates high normal force and hence surface finish deteriorates. SR increases with increase in the pulse-on time. The increase in the pulse-on time increases the time available for the heat to sink into the workpiece, which results in more thermal softening. This softening of the workpiece reduces attrition wear of the grit, which in turn, results in higher protrusion height, and hence higher depth of penetration so a bigger crater is formed in the workpiece surface, so SR increases.

Table 9 Optimization and confirmation results

Responses	Initial setting of control factors	Optimum setting of control factors	Initial value	Optimum values		Improvement (%)
				Prediction	Experimentation	
MRR (g/min)	$x_{11}\ x_{21}\ x_{31}\ x_{41}$	$x_{13}\ x_{23}\ x_{31}\ x_{41}$	0.0640	0.1183	0.1194	95.46
SR (μm)	$x_{11}\ x_{21}\ x_{31}\ x_{41}$	$x_{11}\ x_{21}\ x_{31}\ x_{44}$	1.10	0.78	0.81	29.09

x_{ij}: j^{th} level of i^{th} control factor

5.2 Optimization

In the present case, the objective function of optimization problem can be stated as below:

Find: x_1,x_2,x_3 and x_4

Minimize:

$$\begin{aligned} SR = {} & 2.3961 - 0.2013x_1 - 0.0103x_2 - 0.0552x_3 - 0.008697x_4 \\ & + 0.03986x_1^2 + 0.000711x_2^2 + 0.001578x_3^2 \\ & + 0.00002182x_4^2 \end{aligned} \quad (8)$$

With range of process input parameters:

$$\begin{aligned} 2 \le x_1 \le 6 \\ 10 \le x_2 \le 30 \\ 15 \le x_3 \le 25 \\ 80 \le x_4 \le 240 \end{aligned}$$

For SR, the population size 20, cross over rate 1.0, mutation rate 0.01, and number of generation of 50 are taken. The objective function in Eq. (8) has been solved without any constraint. In Fig. 7, the best and mean fitness curves are illustrated in the search space. The fitness function is optimized when the mean curve converges with the best curve after 10 generations. The corresponding values of control factors peak current, pulse-on time, pulse-off time, and grit number have been found as 2.83 A, 10 μs, 15.20 μs, and 210, respectively. Hence, these are the optimum values of control factors. Using these values, the value of SR has been obtained as 0.78 μm.

The confirmation experiments have also been performed at predicted optimum level of control factors and shown in Table 9. The experimental results of MRR and SR shown in this Table are the average of three trials at the optimum levels. The comparison of optimum results with that of results obtained at initial level of control factors show considerable improvement in MRR and surface finish.

6 Conclusions

The development of EDDFG setup for machining copper–iron–graphite MMC and further process modeling and optimization results use a hybrid approach of response surface model and genetic algorithm shows that:

(1) The developed setup is performing according to planned goals.
(2) The developed response surface models for MRR and SR have been found adequate. The linear and square terms are found significant for MRR model while only square terms are significant for SR model.
(3) The peak current and grit size of diamond wheel have been identified as the most significant control factors for MRR while peak current and pulse-on time have been identified as significant factors for SR.
(4) The MRR has been found to increase with the increase of peak current or decrease of grit number. The SR has increasing trend with the increase in peak current or pulse-on time.
(5) Optimization results show improvements of 95 and 29 % in MRR and SR, respectively.

References

1. Garg RK, Singh KK, Sachadeva A, Sharma V, Ojha K (2010) Review of research work in sinking EDM and WEDM on metal matrix composite materials. Int J Adv Manuf Technol 50:611–624. doi:10.1007/s00170-010-2534-5
2. Karl UK (2006) Metal matrix composites: custom-made materials for automotive and aerospace engineering. WILEY-VCH, New York
3. Jain VK (2002) Advanced machining processes. Allied Publishers, New Delhi
4. Pandey PC, Shan HS (1997) Modern machining processes. Tata McGraw-Hill Publishing Company Ltd, New Delhi
5. Ozgedik A, Can C (2006) An experimental investigation of tool wear in electric discharge machining. Int J Adv Manuf Technol 27:488–500. doi:10.1007/s00170-004-2220-6
6. Kansal HK, Singh S, Kumar P (2005) Parametric optimization of powder mixed electric discharge machining by response surface methodology. J Mater Process Technol 169:427–436. doi:10.1016/j.jmatprotec.2005.03.028
7. Lauwers B, Kruth JP, Lin W, Eeraerts W, Schacht B, Bleys P (2004) Investigation of material removal mechanisms in EDM of composite ceramic materials. J Mater Process Technol 149:347–352. doi:10.1016/j.jmatprotec.2004.02.013
8. Ramulu M, Paul G, Patel J (2001) EDM surface effect on the fatigue strength of a 15 vol% SiC_p/Al metal matrix composite material. Compos Struct 54:79–86. doi:10.1016/s0263-8223(01)00072-1
9. Mohan B, Rajadurai A, Satyanarayana KG (2004) Electric discharge machining of Al-SiC metal matrix composites using rotary

tube electrode. J Mater Process Technol 153–154:978–985. doi:10.1016/j.jmatprotec.2004.04.347
10. Ji RJ, Liu YH, Zhang YZ, Wang F, Cai BP, Li H (2012) Compound machining of silicon carbide ceramics by high speed end electrical discharge milling and mechanical grinding. Chin Sci Bull 57(4):421–434. doi:10.1007/s11434-011-4822-3
11. Ji RJ, Liu YH, Zhang YZ, Wang F, Cai BP, Li H, Ma J (2010) Optimizing machining parameters of silicon carbide ceramics with ED milling and mechanical grinding combined process. Int J Adv Manuf Technol 51(1–4):195–204. doi:10.1007/s00170-010-2628-0
12. Ji RJ, Liu YH, Zhang YZ, Wang F, Cai BP, Li H, Dong X (2012) Machining performance optimization in end ED milling and mechanical grinding compound process. Mater Manuf Process 27(2):221–228. doi:10.1080/10426914.2011.568569
13. Ji RJ, Liu YH, Zhang YZ, Wang F, Li H, Cheng XD (2010) Machining performance and surface integrity of SiC ceramic machined using electrical discharge milling and the mechanical grinding compound process. Proc IME B J Eng Manufact 224(10):1511–1518. doi:10.1243/09544054JEM1863
14. Jain VK, Choudhary SK, Gupta M (1999) Electrical discharge diamond grinding of high speed steel. Machi Sci Technol 3(1):91–105. doi:10.1080/10940349908945685
15. Koshy P, Jain VK, Lal GK (1996) Mechanism of material removal in electrical discharge diamond grinding. Int J Mach Tools Manuf 36:1173–1185. doi:10.1016/0890-6955(95)00103-4
16. Kumar S, Choudhury SK (2007) Prediction of wear and surface roughness in electrodischarge diamond grinding. J Mater Process Technol 191(1):206–209
17. Chandrasekhar BA, Yadava V, Singh GK (2010) Development and experimental study of electro-discharge face grinding. Mater Manuf Process 25:1–6. doi:10.1080/10426910903367436
18. Koshy P, Jain VK, Lal GK (1999) Grinding of cemented carbide with electrical spark assistance. J Mater Process Technol 72:61–68. doi:10.1016/S0924-0136(97)00130-1
19. Singh GK, Yadava V, Kumar R (2010) Diamond face grinding of WO-CO composite with spark assistance: experimental study and parameter optimization. Int J Precis Eng Manuf 11(4):509–518. doi:10.1007/s12541-010-0059-3
20. Shrivastava A, Dubey AK, Shrivastava PK (2012) Computer-aided hybrid ANN-GA approach for modeling and optimization of EDDG process. Int J Abra Technol 5:245–257. doi:10.1504/IJAT.2012.051034
21. Phadke MS (1989) Quality engineering using robust design. Prentice-Hall, Englewood Cliffs
22. Montgomery DC (1997) Design and analysis of experiments. Wiley, New York
23. Deb K (1995) Optimization for engineering design: algorithms and examples. Prentice-Hall of India Pvt Ltd, New Delhi
24. Lamba VK (2008) Neuro fuzzy systems. University Science Press, New Delhi
25. Rao PN (2004) Manufacturing technology-metal cutting and machine tools. Tata McGraw-Hill Publishing Company Limited, New Delhi